

# Progress in solid acid fuel cell electrodes

Aron Varga

Leibniz Institute of Surface Modification, Permoserstraße 15, D-04318 Leipzig, Germany

## Email address:

[aron.varga@iom-leipzig.de](mailto:aron.varga@iom-leipzig.de)

## To cite this article:

Aron Varga. Progress in Solid Acid Fuel Cell Electrodes. *American Journal of Nano Research and Application*. Special Issue: Advanced Functional Materials. Vol. 2, No. 6-1, 2014, pp. 61-65. doi: 10.11648/j.nano.s.2014020601.18

**Abstract:** Solid acid fuel cells represent a relatively new technology with the advantage of an intermediate operating temperature of 240°C and a solid state proton conducting electrolyte ( $\text{CsH}_2\text{PO}_4$ ). Widespread commercial application has been hindered mainly by low performance and costly electrodes containing a high Pt loading. Here we review the recent progress and current status of solid acid fuel cell electrodes. Major efforts include creating nanostructured composites leading to much reduced Pt loadings while maintaining or even increasing performance. Furthermore, fundamental studies on Pt thin films, as geometrically controlled electrodes, have recently revealed the possibility of an electrochemical pathway through the two-phase boundary in addition to the classic three-phase boundary. Carbon nanotubes as electronic interconnects have been shown to dramatically improve Pt catalyst utilization and hence electrode performance. Major efforts are spent to search for alternative, non-precious metal catalysts.

**Keywords:** Solid Acid Fuel Cells, Electrodes,  $\text{CsH}_2\text{PO}_4$ , Pt, CNTs

## 1. Introduction

Fuel cells have been heralded as the energy technology of the future for many decades. Start-up companies, industrial giants, government supported pilot programs came and went periodically causing boom and bust periods. Despite multiple disappointments, the technology is just too elegant and attractive to be abandoned altogether, and here, a highly promising, new class of fuel cell is regarded. Especially in the light of an ever increasing necessity for efficient energy storage and conversion devices, fuel cells are becoming more important since they can most efficiently convert chemical energy to electrical and vice versa. Since their invention in the 19<sup>th</sup> century, multiple technologies have been developed, with most efforts spent on the portable and flexible low temperature technology based on polymer electrolytes (PEMFCs) and the stationary but highly efficient technology based on solid oxide materials (SOFCs). A relative newcomer in this field is the solid acid fuel cell (SAFC), based on the solid acid material  $\text{CsH}_2\text{PO}_4$ [1]. Their intermediate operating temperature of 240°C and a truly solid state electrolyte provide multiple technological advantages, such as the suitability of stainless steel interconnects, fuel flexibility and resistance to catalyst poisoning. However, widespread commercial application has been hindered by the need for relatively high loadings of precious metal Pt as the electrocatalyst and low electrode performance[2]. Here we

review recent progress and current status of solid acid fuel cell electrodes.

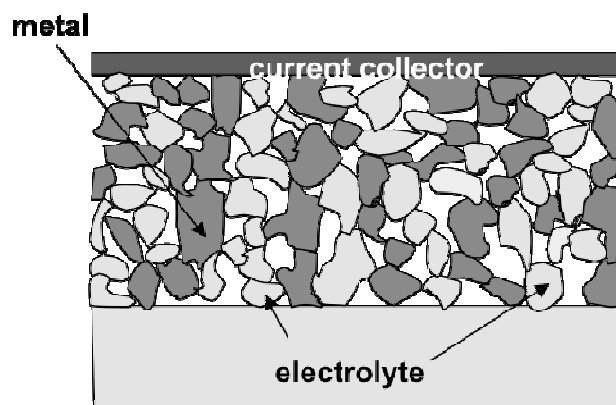


**Figure 1.** Schematic of a solid acid fuel cell electrode consisting of porous, interconnected Pt catalyst and  $\text{CsH}_2\text{PO}_4$  electrolyte particles[3].

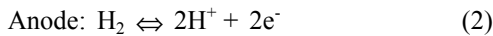
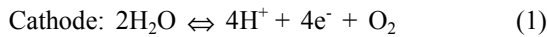
In general, SAFCs employ a pure ion conducting electrolyte (no electron-ion mixed conductivity as with some solid oxide fuel cell electrode materials) and Pt as the electrocatalyst. The electrochemical reactions occur where the simultaneous transport of ions, electrons and gas molecules is possible, i.e. the so-called triple phase boundary between the electrolyte, the catalyst and the gas phase, Fig 1[3]. Considering these restrictions, the ideal electrode consists of an interpenetrating, 3-dimensional, interconnected

structure of the electrolyte and the electrocatalyst with high porosity for gas access.

As with other low and intermediate temperature fuel cells, the overpotential at the cathode is far greater than that at the anode and with electrolyte membranes as thin as 20  $\mu\text{m}$ , the overpotential due to Ohmic ion transport resistance can be neglected[4].

## 2. Electrochemical Measurements of Electrodes

The most convenient method to measure the electrochemical performance of solid acid fuel cell electrodes is AC impedance spectroscopy in a single chamber, symmetric gas environment. Such a measurement does not require complicated and error-prone sealing but allows a detailed analysis of the electrode reaction kinetics as well as separation of the electrolyte response. However, such symmetric cell measurements are limited to hydrogen (hydrated to  $\text{pH}_2\text{O} = 0.4$  atm to prevent dehydration of the electrolyte[5]) since Pt is in its oxidized form in thermodynamic equilibrium in an oxygen gas environment at ca. 240°C. Despite this challenge, the anode performance is often assumed to be indicative for cathode performance, since the same geometric features, namely the triple phase boundary, is rate limiting for both the oxygen reduction and the hydrogen oxidation reaction. A high performance anode is also a high performance cathode with this material system. During a symmetric cell measurement, the forward and the reverse electrochemical reaction is captured simultaneously and it is assumed that the electrochemical impedance contribution is equal in magnitude:



In order to uniquely separate the electrode impedance for a specific reaction, such as the hydrogen oxidation, a reference electrode is traditionally used. However, it has been shown by Adler[6] that in a solid state system, the placement of the reference electrode is extremely sensitive, potentially introducing a large error in the measurement. An elegant solution to this problem has been described by Sasaki et. al.[7], suggesting to geometrically restrict the working electrode such that its overpotential becomes dominant, in a reference electrode free configuration, Fig 2. The impedance of the much larger counterelectrode can be neglected. A quantitative relationship between the size ratio of the electrodes (working electrode radius:  $r_{\text{we}}$  and counter electrode radius:  $r_0$ ) and the electrolyte thickness ( $t$ ) where the electrode responses are well separated, was established through a computational and experimental study.

AC impedance spectroscopy of electrochemical cells with an asymmetric geometry permit, with a suitable size ratio of the working electrode and the counter electrode, the measurement of the cathodic reaction in a symmetric oxygen

environment. Thermochemical considerations reveal that at the SAFC operating temperature of 240°C and at 0.6 atm  $\text{pO}_2$ , the standard free energy of formation of PtO is ca. -22 kJ/mol.[8] Hence a voltage of at least 0.22 V across the electrode shifts the equilibrium of the oxidation reaction in favor of Pt. This implies that for an electrochemical cell with an asymmetric geometry ( $t = 3$  mm,  $r_0 = 1$  cm, and  $r_{\text{WE}} = 1$  mm) an electric DC bias of 0.3 V is sufficient to access the electrochemical activity of Pt in its reduced form. The overpotential across the electrolyte film and the counter electrode, even when its specific activity as PtO is lower than that of Pt, is negligible.

## 3. Composite Solid Acid Fuel Cell Electrodes

### 3.1. Microstructured Powder Electrodes

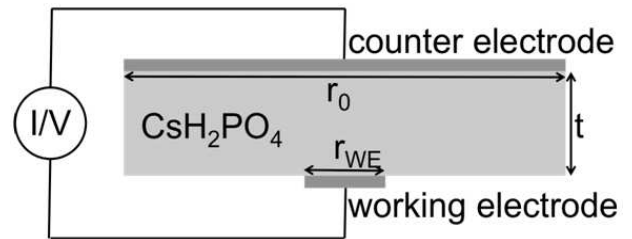


**Figure 2.** Schematic of an electrochemical cell with asymmetric geometry and symmetric gas configuration for AC impedance spectroscopy.

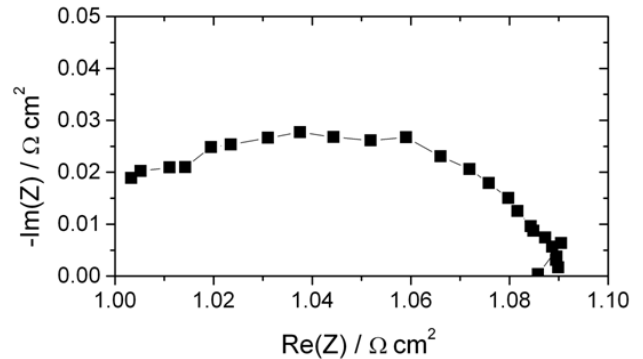


**Figure 3.** Nyquist plot of the electrode impedance for symmetric cell with powder electrodes ( $\text{CsH}_2\text{PO}_4$ : Pt : Pt/C = 3 : 3 : 1 weight ratio) measured at 240°C in humidified hydrogen.

The first generation solid acid fuel cell electrodes consisted of a composite powder of  $\text{CsH}_2\text{PO}_4$  microparticles, Pt and Pt on carbon nanoparticles, mixed with the pore former naphthalene [4,9]. An intimate mixture of the components is achieved with ultrasonication as a suspension in toluene and subsequent drying, ballmilling, or grinding with mortar and pestle. The membrane electrode assembly is obtained by co-pressing the electrode powder mix with a uniaxial cold-press with a layer of pure  $\text{CsH}_2\text{PO}_4$  as the electrolyte at 34 MPa. Upon heating to the operating temperature of 240°C, the electrolyte particles partially sinter and ensure a continuous ion transport from the catalytically active centers to the electrolyte membrane. The large difference in the

particle sizes and the mechanical properties of the electrolyte and the electrocatalyst, as well as the complete decomposition of naphthalene ensures that continuous pores remain for gas access. With a Pt loading of  $7.7 \text{ mg/cm}^2$ , the to-date lowest published electrode resistance of  $0.06 \Omega \text{ cm}^2$  was obtained, and here successfully reproduced, Fig. 3. Nevertheless, the Pt mass normalized activity of such electrode with  $2.2 \text{ S/mg}$  is low, implying that the spatial distribution of the catalyst is suboptimal. Not all catalyst particles are connected with the electrolyte or electronically connected to the current collector. From simple geometric considerations, an improved matching of the electrolyte and electrocatalyst particle size leads to improved catalyst distribution and hence utilization. It has been shown experimentally that mechanical mixtures of composite electrode powders with decreasing electrolyte particle sizes indeed result in lower electrode overpotentials[2].

### 3.2. Nanostructured Electrodes via Electrospray

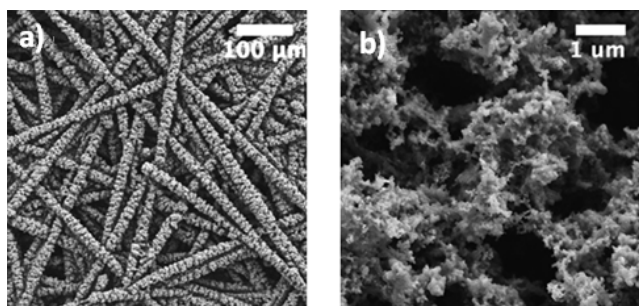


**Figure 4.** Scanning electron micrograph of nanocomposite SAFC electrode ( $\text{CsH}_2\text{PO}_4$  and Pt nanoparticles at (a) low and (b) high magnification, deposited onto carbon paper via electrospray [10].

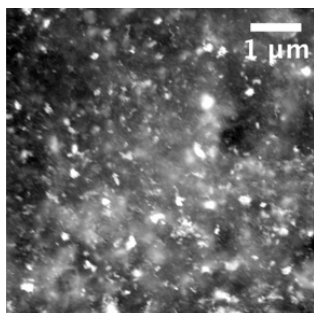


**Figure 5.** Scanning electron micrograph of nanocomposite SAFC electrode ( $\text{CsH}_2\text{PO}_4$ , Pt) obtained with a back scattered electron detector, showing isolated Pt particles as bright areas.

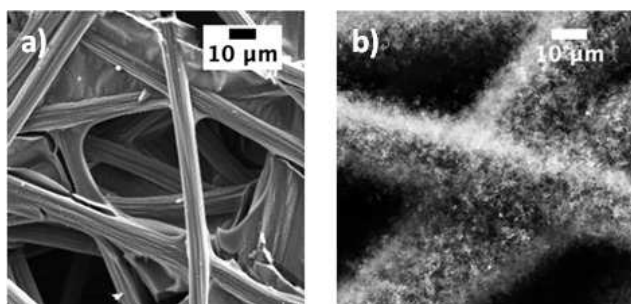


**Figure 6.** Scanning electron micrographs of (a) blank carbon paper and (b) CNT overgrown carbon paper.

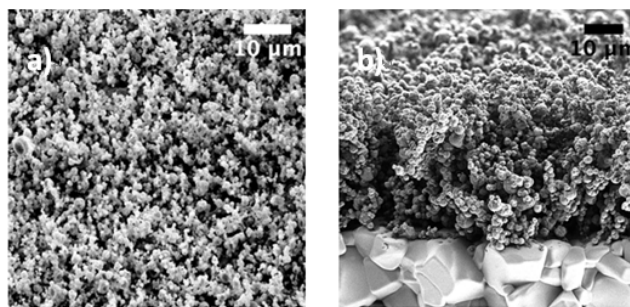


**Figure 7.** Scanning electron micrographs of SAFC electrode deposited via spraydrying onto a  $\text{CsH}_2\text{PO}_4$  electrolyte pellet (a) top-view; (b) side view.

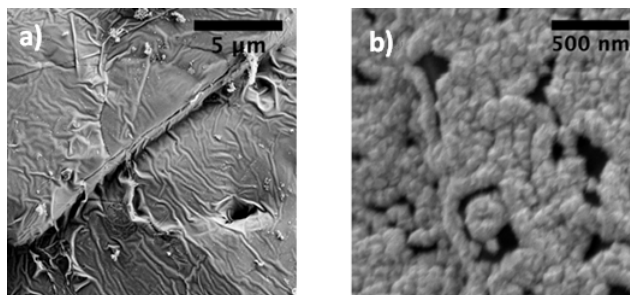


**Figure 8.** Scanning electron micrographs of SAFC electrode WITH Pt deposited via metal organic chemical vapor deposition (MOCVD) onto a  $\text{CsH}_2\text{PO}_4$  electrolyte pellet at (a) low; (b) high magnification.

Substantial efforts have been spent on reducing the electrolyte particle size to the sub-micron regime. The aim is to increase the density of electrochemically active triple phase boundaries between the  $\text{CsH}_2\text{PO}_4$  electrolyte, the Pt electrocatalyst nanoparticles (ca. 10nm diameter for commercially available standard catalysts) and the gas phase, by improving the catalyst distribution. The challenges for  $\text{CsH}_2\text{PO}_4$  particle size reduction stem from the fact that  $\text{CsH}_2\text{PO}_4$  is a hygroscopic material with a low melting point and thus is prone to agglomeration. As an in-situ nanoparticle fabrication method, without the need for post-synthesis particle processing, electrospray deposition does indeed allow the production of sub-micron  $\text{CsH}_2\text{PO}_4$  particles. When directly deposited onto a substrate, an interconnected, highly porous electrolyte structure with a feature size of down to 100 nm can be created[10]. In addition, the electrocatalyst can be co-deposited when suspended in the electrospray precursor solution, Fig. 4. Further additives, such as the polymer polyvinylpyrrolidone (PVP) stabilize the otherwise unstable nanostructure even under fuel cell operating conditions. With  $0.3 \text{ mg/cm}^2$ , a substantial reduction of the catalyst loading has been achieved without sacrificing electrode performance, when compared to mechanically mixed electrodes[7].

However, the mass normalized activity of  $2.2 \text{ S/mg Pt}$  is similar to the values obtained with the mechanically mixed electrodes. Scanning electron micrographs taken with a backscattered electron detector show isolated Pt nanoparticles, Fig. 5, and hence indicate that the loss of electronic interconnectivity between the catalyst nanoparticles and agglomeration in the precursor solution is the main cause of the low mass normalized activity. In addition, a major drawback of electrospray synthesis is the low deposition rate

of 5 mg/h.

To improve the electronic interconnectivity of Pt catalyst nanoparticles, without increasing the Pt loading, carbon nanotubes (CNTs) have been grown directly onto the standard current collector, carbon paper via chemical vapor deposition (CVD). The matching size scales of the current collector (CNT + carbon paper) and the feature size of the electrosprayed nanostructure result in a higher statistical likelihood of a Pt nanoparticle to be connected with the CNT (20–40 nm diameter), compared with a bare carbon fibers (10  $\mu\text{m}$  diameter) from the carbon paper, Fig. 6. The mass normalized activity thus was improved 3-fold to 6.6 S/mg and the stability was demonstrated with AC impedance measurements with a DC voltage bias [11].

### 3.3. Nanostructured Electrodes via Spraydrying

Spraydrying has been explored as a more easily scalable method compared to electrospray and hence technologically more relevant process, to obtain nanostructured solid acid fuel cell electrodes[12]. Here, an aerosol is generated via a vibrating mesh membrane with micron sized  $\text{CsH}_2\text{PO}_4$  solution droplets. The droplets are carried by a heated gas stream to an electrophoretic deposition area. During flight, the solvent evaporates and the solute precipitates to form nanoparticles, with the size mainly depending on the concentration. Ultimately, a diffusion limited aggregate is deposited on a given substrate, such as carbon paper current collector, or prefabricated electrolyte pellet, with a feature size similar to electrosprayed structures, Fig. 7. A deposition rate of 165 mg/h can be achieved covering a surface area of 1750  $\text{cm}^2$ . The Pt electrocatalyst was added via sputtering. The electrode impedance was 3.6  $\Omega\text{ cm}^2$  and a mass normalized activity of 13 S/mg was obtained.

## 4. Thin Film Electrodes

### 4.1. Sputtered Thin Film Electrodes

In contrast to high performance, nanocomposite structures, simple, geometrically controlled electrodes in the form of a thin films, deposited onto a polished electrolyte pellet, allow fundamental studies of the rate-limiting step of electrochemical reactions. Careful analysis of such electrodes by Louie and Haile[13], with systematically varying film thickness and outer diameter reveal that for sub-50 nm Pt films, obtained by DC magnetron sputtering, a significant contribution to the electrode performance is via the two-phase boundary between the electrocatalyst and the electrolyte. Here the reaction rate is not limited by the diffusion process of dissociated hydrogen across the metal thin film. In addition, a lower bound for the specific activity of the triple phase boundary was estimated to be 41 k $\Omega\text{ cm}$ . A remarkable mass normalized activity of 19 S/mg and an area normalized electrode impedance of ca. 3.1  $\Omega\text{ cm}^2$  was measured with Pt films of 7.5 nm thickness. Due to its significantly higher hydrogen permeability, Pd is expected to play an important role in high performance thin film electrodes[14], such as

Pt-Pd-Pt sandwich structure.

### 4.2. Thin Film Electrodes via MOCVD

Pt particles or thin films can be obtained via metal organic chemical vapor deposition (MOCVD), using  $\text{Pt}(\text{acac})_2$  as the precursor material[15]. Here, the metal organic compound is mixed with  $\text{CsH}_2\text{PO}_4$  powder and heated to at least 150°C in a vacuum oven that has been evacuated and purged with nitrogen. Water that keeps  $\text{CsH}_2\text{PO}_4$  from dehydration may also assist in the decomposition of the metal organic compound on the acidic material surfaces. Thus, conformal Pt coatings can be obtained in a single step, batch synthesis method, Fig. 8, providing a significant advantage over line of sight deposition methods, such as sputtering. Precise control of the film thickness is not difficult, as it can be adjusted either by the amount of  $\text{Pt}(\text{acac})_2$  mixed with  $\text{CsH}_2\text{PO}_4$  powder or by the number of successive depositions. An area normalized impedance of 0.3  $\Omega\text{ cm}^2$  was measured with a Pt loading of 1.8  $\text{mg/cm}^2$ , i.e. with a mass normalized activity of ca. 1.9 S/mg.

## 5. Conclusion and Prospects

Solid acid fuel cells represent a highly attractive technology because of their intermediate operating temperature, considered as the “sweet spot” for fuel cells. About ten years of research and development has shown the tremendous potential in terms of performance and cost. With equivalent catalyst utilization as with PEMFCs, a much higher fuel cell power density can be expected due to the 240°C operating temperature for  $\text{CsH}_2\text{PO}_4$  based electrolytes.

A summary of the main electrode developments is given in table 1. A combination of high surface area electrode and fine distribution of Pt catalyst should lead to an even higher mass normalized activity and lower area specific electrode resistance than the current state of the art. Compared to other fuel cell technologies, such as PEMFCs and SOFCs, the initial relatively competitive 417  $\text{W/cm}^2$  [16] fuel cell power density is projected to surpass current state of the art, upon optimizing the cathode performance. Assuming negligible electrode overpotential and a 10  $\mu\text{m}$  electrolyte membrane, a 2500  $\text{W/cm}^2$  power density can be calculated when using hydrogen and oxygen as the fuel.

Furthermore, alternative, non-precious metal catalyst materials are needed to allow further necessary raw material cost reduction, before widespread technological applicability is possible. The challenge here is the general reactivity of many common metal and metaloxide candidate materials with the electrolyte  $\text{CsH}_2\text{PO}_4$  and the generation of non-conducting, new phases as the reaction product. Here, functionalized, carbon based materials may provide an interesting research direction.

## Acknowledgements

Financial support was provided by the ESF Forschergruppe “Applied and theoretical molecular electrochemistry as a key for new technologies in the area of energy conversion and

storage”.

**Table 1.** Comparison of solid acid fuel cell anodes measured between 238 and 250°C

Electrodes	Electrode resistivity (Ohm cm <sup>2</sup> )	Pt loading (mg/cm <sup>2</sup> )	Mass normalized activity (S/mg)
Pt:Pt/C:CsH <sub>2</sub> PO <sub>4</sub> (3 : 1 : 3 wt) – mech. mix[9,17]	0.06	7.7	2.2
Pt : CsH <sub>2</sub> PO <sub>4</sub> (1 : 2 wt) – mech. mix[7]	1.7	10	0.06
Pt : CsH <sub>2</sub> PO <sub>4</sub> (1 : 2 wt) – electrosprayed[10]	1.5	0.3	2.2
Pt : CsH <sub>2</sub> PO <sub>4</sub> : CNT – electrosprayed[11]	0.5	0.3	6.6
10 nm Pt film, spraydried CsH <sub>2</sub> PO <sub>4</sub> [12]	3.6	0.021	13.2
7.5 nm Pt film, polished CsH <sub>2</sub> PO <sub>4</sub> [13]	3.1 ± 0.5	0.017	19

## References

- [1] S. M. Haile, D. A. Boysen, C. Chisholm, and R. Merle, *Nature* 410, 910 (2001).
- [2] C. R. I. Chisholm, D. A. Boysen, A. B. Papandrew, S. K. Zecevic, S. Cha, K. A. Sasaki, Á. Varga, K. P. Giapis, and S. M. Haile, *Interface Magazine* 18, 53 (2009).
- [3] M. Louie, California Institute of Technology, 2011
- [4] T. Uda and S. M. Haile, *Electrochemical and Solid-State Letters* 8 (5), A245 (2005).
- [5] A. Ikeda, S. M. Haile, *Solid State Ionics* 213, 63 (2012)
- [6] S. B. Adler, *Journal of The Electrochemical Society* 149 (5), E166 (2002).
- [7] K. A. Sasaki, Y. Hao, and S. M. Haile, *Physical chemistry chemical physics : PCCP* 11 (37), 8349 (2009).
- [8] K. Ota and Y. Koizumi, in *Handbook of Fuel Cells - Fundamentals, Technology and Applications*, edited by W. Vielstich, H. Yokokawa, and H. A. Gasteiger (John Wiley and Sons, 2009), Vol. 5, pp. 243.
- [9] S. M. Haile, C. R. I. Chisholm, K. Sasaki, D. A. Boysen, and T. Uda, *Faraday Discussions* 134, 17 (2007).
- [10] Á. Varga, N. A. Brunelli, M. W. Louie, K. P. Giapis, and S. M. Haile, *Journal of Materials Chemistry* 20 (30), 6309 (2010).
- [11] Á. Varga, M. Pföhl, N. A. Brunelli, M. Schreier, K. P. Giapis, and S. M. Haile, *Physical chemistry chemical physics : PCCP* 15 (37), 15470 (2013).
- [12] R. C. Suryaprakash, F. Lohmann, M. Wagner, B. Abel, and A. Varga, *RSC Adv.* (2014).
- [13] M. W. Louie and S. M. Haile, *Energy & Environmental Science* 4 (10), 4230 (2011).
- [14] M. W. Louie, K. Sasaki, and S. M. Haile, *ECS Transactions* 13 (28), 57 (2008).
- [15] A. B. Papandrew, C. R. I. Chisholm, R. A. Elgammal, M. M. Özer, and S. K. Zecevic, *Chemistry of Materials* 23 (7), 1659 (2011).
- [16] T. Uda, D. A. Boysen, C. R. I. Chisholm, and S. M. Haile, *Electrochemical and Solid-State Letters* 9 (6), A261 (2006).